ROYAL SOCIETY
OF CHEMISTRY

PAPER

Concurrent determination of U, Np, Pu, Am, and Cm in clay systems at ultra-trace levels with accelerator mass spectrometry†

Daniel Glückman, ID *[a] Francesca Quinto, ID [a] Karin Hain,[b] Claudia Joseph, ID [a]
Vanessa Montoya, ID [ac] Peter Steier[b] and Horst Geckeis[a]

The geochemistry of actinides under reducing conditions in a deep geological nuclear waste repository is characterized by low solubility and strong sorption to mineral surfaces. The quantification of actinide migration (*i.e.* diffusion) at resulting concentration levels requires an analytical method able to determine actinide concentrations down to ultra-trace levels ($\approx$ fg g^{-1}). In the actual study, such an analytical procedure was tested by using accelerator mass spectrometry (AMS), one of the very few analytical techniques that can presently meet those requirements. Specimens simulating the sample matrix representative for a diffusion experiment in natural clay rock were produced by spiking clay rock powders (Opalinus Clay or Callovo-Oxfordian Clay) and aliquots of corresponding pore waters with the actinide nuclides ^{233}U, ^{237}Np, ^{244}Pu, and ^{248}Cm in amounts ranging from approximately 3×10^{-19} to 5×10^{-15} mol per sample ($\approx$ 0.07–1000 fg per sample). The actinide nuclides were separated as group *via* Fe(OH)$_3$ co-precipitation and then analyzed sequentially with AMS. During such analysis a decrease in count rates by up to a factor of 6 was observed in high-matrix clay rock samples compared to low-matrix standard solutions. Since the chemical yield of the actinides in the Fe(OH)$_3$ co-precipitation step prior to analysis turned out to be quantitative, this observation must originate from a reduction of the sputter rate of the actinide nuclides in the AMS ion source, which can be described partly as a dilution effect. By determining chemical-ionization-yield factors, suitable non-isotopic tracers were identified for ^{237}Np and ^{243}Am. This allowed for the concurrent determination of all actinide nuclides at levels down to 3×10^{-19} mol per sample. Different actinides in a deep geological formation may be present in concentration ranges differing by orders of magnitude depending on their chemical form and solubility. Such concentration spreads were simulated by preparing clay rock/pore water samples where each individual sample contained ^{233}U, ^{237}Np, ^{244}Pu, ^{243}Am, and ^{248}Cm at quantities ranging from approximately 3×10^{-19} to 4×10^{-15} mol per sample. The presented sample preparation procedure, in combination with the extraordinary detection sensitivity of AMS allows for the simultaneous determination of diffusion profiles of several actinides at ultra-trace levels within one experiment.

1 Introduction

Clay rock is a potential host rock for the final disposal of high-level nuclear waste (HLW) in deep geological formations. It is expected that under reducing conditions of the clay rock/pore water system actinides potentially released from radioactive waste forms exhibit low solubility and undergo strong sorption.

Consequently, actinide species in their reduced oxidation state are expected to be rather immobile, and diffusion as the main transport mechanism in clay rock will be very slow. An analytical method able to determine actinides down to ultra-trace levels ($\approx$ fg g^{-1}) is needed to experimentally examine such anticipated diffusion profiles. One of the most sensitive analytical techniques for the determination of rare, long-lived actinides in natural samples is accelerator mass spectrometry (AMS). At the Vienna Environmental Research Accelerator (VERA), the overall detection efficiency, measured as unambiguous ^{236}U events in the detector per atom of ^{236}U in the sample, is equal to approximately 2.2×10^{-4} counts in environmental samples.[1] Such sensitivity allows for the determination of actinide nuclides down to quantities of ag per sample or 10^{-19} mol per sample without previous chemical separation

ᵃKarlsruhe Institute of Technology (KIT), Institute for Nuclear Waste Disposal (INE), Hermann-von-Helmholtz-Platz 1, 76344 Eggenstein-Leopoldshafen, Germany. E-mail: daniel.glueckman@kit.edu

ᵇFaculty of Physics, University of Vienna, Währinger Straße 17, 1090 Vienna, Austria

ᶜEngineered and Geosystems Analysis, Expert Group Waste & Disposal, Institute for Environment, Health and Safety, Belgian Nuclear Research Centre - SCK CEN, 2400 Mol, Belgium

from each other, and in the presence of naturally occurring uranium.[2,3]

The present study aimed at the testing of a highly sensitive method for the analysis of actinides in clay systems by applying AMS and for the simultaneous determination of different actinides in the same clay sample. There are various issues to be tackled for such multi-actinide analyses. Particularly challenging is the choice of yield tracers with a sufficient degree of isotopic purity, as well as the non-availability of isotopic tracers for ^{237}Np and ^{243}Am.[2] The use of carefully chosen isotopic and non-isotopic tracers has already been reported to allow for the concurrent AMS measurement of several actinides in one sample and was applied to granitic groundwater samples from the Grimsel Test Site in Switzerland.[2,3] In these studies, a group separation of the actinides from the sample matrix via Fe(OH)$_3$ co-precipitation was performed with the use of ^{239}Pu and ^{248}Cm as non-isotopic tracers for the determination of ^{237}Np and ^{243}Am, respectively. These groundwater samples featured a low ionic strength ($\approx 10^{-3}$ mol L^{-1}) and therefore had a low matrix content. However, clay rock samples present a significantly more complex matrix that can have an impact on the performance of the chemical procedure, as well as on the analysis with AMS.

In the actual work, the multi-actinide analysis with AMS was tested with clay rock and clay pore water matrices of Opalinus Clay (OPA) and Callovo-Oxfordian Clay (COx). Both clay rock formations are investigated as reference host rocks for the disposal of highly radioactive waste in Switzerland and France, respectively. Before testing the analytical method for different relevant concentration levels of U, Np, Pu, Am, and Cm, solubility and speciation calculations for the five studied actinides under reducing conditions were performed with the software PHREEQC v.3.[4]

In detail, the following steps were performed: (i) testing of the sensitivity of the analytical method for the determination of U, Np, Pu, and Cm in OPA and COx, (ii) the concurrent determination of U, Np, Pu, Am, and Cm with concentrations ranging from 3×10^{-19} to 4×10^{-15} mol per sample, reflecting their expected relative concentrations, in OPA and COx, and the corresponding pore waters within diffusion experiments, (iii) determination of the suitability of ^{244}Pu and ^{248}Cm as non-isotopic tracers for ^{237}Np and ^{243}Am, respectively, in clay matrix samples, and (iv) investigation of the influence of the sample matrix on the efficiency of the analytical procedure.

2 Experimental

2.1 Materials

Standard solutions of ^{233}U (IRM-040/1), ^{237}Np (Eckert & Ziegler P.O. No P701765), ^{244}Pu (IRM-042a), and ^{243}Am (Eckert & Ziegler P.O. No P624735), and an in-house solution of ^{248}Cm were gravimetrically diluted down to approximately 3.3×10^{-12} mol L^{-1} to be used as actinide tracers. All dilutions and solutions used in the sample preparation, as well as in the cleaning of the vessels were prepared with ultra-pure water from a Milli-Q® Advantage A10 water purification system (18.2 MΩ cm (22 ± 1) °C; Merck Millipore, Darmstadt,

Germany). Nitric acid (65%, ultrapure grade, Roth, Karlsruhe, Germany), hydrochloric acid (34%, ultrapure grade, Roth, Karlsruhe, Germany), ammonia solution (25%, Suprapur®, Merck, Darmstadt, Germany), and iron powder (99.99%, metals basis, Alfa Aesar™, Puratronic™, Fisher Scientific, Schwerte, Germany) were employed as reagents during sample preparation.

OPA (borehole BLT-14) was obtained from the underground research laboratory (URL) in Mont Terri located in St. Ursanne, Switzerland,[5] while COx (borehole EST 104) originated from the URL in Meuse/Haute-Marne in Bure, France.[6] The clay rock samples were ground to fine powders by using a metal blade (Hoffmann SE, München, Germany).

Synthetic OPA and COx pore waters were prepared as described by Pearson et al. (1998),[7] with a pH of 7.6 and an ionic strength of 0.36 mol L^{-1} and by Savoye et al. (2015),[8] with a pH of 7.4 and an ionic strength of 0.33 mol L^{-1}, respectively.

2.2 Solubility and speciation calculations

In order to estimate the solubility limit of the investigated actinides in OPA and COx pore water under repository conditions, solubility and speciation calculations were carried out with PHREEQC v.3,[4] using the ThermoChimie v.10 database,[9] including ionic strength corrections using the specific ion interaction theory (SIT) approach.

The geochemical parameters of OPA and COx pore waters used for the calculations, such as elemental composition, pH, and E_h were based on the characterization of natural pore waters and are shown in ESI Table S1.† For OPA pore water, the elemental composition was obtained from Gautschi (2017),[10] with a pH of 7.5, an ionic strength of 0.23 mol L^{-1}, and an E_h of −185 mV. The elemental composition of COx pore water is described by Vinsot et al. (2008),[11] with a pH of 7.2, an ionic strength of 0.32 mol L^{-1}, and an E_h of −200 mV.

The relative concentrations of the actinides (Table 2) obtained from these speciation calculations served for the preparation of the samples in the actual experiment and for the identification of the most relevant chemical parameters affecting the studied system. The calculated solid phases of the five actinides and their corresponding dominant aquatic species in the two pore waters are shown in ESI Table S2.†

2.3 Sample description

In order to simulate specimens obtained from a clay rock diffusion experiment,[12] three types of sample series were prepared containing the actinide nuclides and one of the following matrices: (a) 100 mg of OPA or COx powder (hereafter referred to as matrix type A); (b) 20 mL of OPA or COx synthetic pore water (hereafter referred to as matrix type B); furthermore, (c) spiked standard solutions, containing 5 mL of 1 mol L^{-1} HNO$_3$, in the absence of clay rock/pore water matrices (hereafter referred to as matrix type C).

These three types of sample series were further grouped into four different sample sets: (i) sensitivity test samples, (ii) concentration test samples, (iii) matrix test samples, and (iv) blank samples. In this way, a total of 20 spiked samples and 10

This journal is © The Royal Society of Chemistry 2022

J. Anal. At. Spectrom., 2022, **37**, 1696–1705 | **1697**

procedural blank samples were obtained, whose compositions are listed in Table 1 and described in more detail in the following paragraphs.

2.3.1   Sensitivity test samples. Five samples of matrix type A for each clay rock were prepared, respectively, resulting in a total of 10 samples. To each sample, the four actinides ^{233}U, ^{237}Np, ^{244}Pu, and ^{248}Cm were added in amounts ranging from approximately 3×10^{-19} to 5×10^{-15} mol per sample. The amount of each actinide added to a particular sample was the same. The aim was to check for the analytical limitations with regard to low concentrations for the individual actinides of interest in different samples, in addition to the determination of the background *via* blank measurements.

2.3.2   Concentration test samples. One sample of matrix type A and one sample of matrix type B were prepared for each clay type, respectively, giving a total of four samples. The five actinide nuclides ^{233}U, ^{237}Np, ^{244}Pu, ^{243}Am, and ^{248}Cm were added in relative amounts ranging from approximately 3×10^{-19} to 4×10^{-15} mol per sample, representing levels of actinides near the expected detection limit of AMS ($\approx 10^{-20}$ mol).[13]

This sample set aimed at simulating specimens obtained from a real actinide diffusion experiment in clay rock where the actinides – due to their different solubilities in clay pore waters (Table 2) – are present at quantities differing by up to four orders of magnitude from each other. The goal was to show that the concurrent ultra-trace determination of the five actinide nuclides, present at such differing quantities, within the same sample target would be possible.

2.3.3   Matrix test samples. One sample of matrix type A, one sample of matrix type B and one sample of matrix type C for each clay type were prepared, respectively (6 samples in total). Approximately 5×10^{-16} mol of each of the five actinide nuclides ^{233}U, ^{237}Np, ^{244}Pu, ^{243}Am, and ^{248}Cm were added to each sample. These samples provided a performance comparison of the analytical procedure among samples of different matrices.

2.3.4   Blank samples. Four procedural blank samples composed of matrix type A (two samples for each type of clay rock) were prepared and measured with AMS for estimation of the background of the actinide nuclides. An additional 6 blank samples of matrix type A (three samples for each type of clay rock) were prepared in order to investigate the efficiency of the Fe(OH)$_3$ co-precipitation with regard to the group separation of the actinides.

2.4   Sample preparation and analysis

For the determination of diffusion profiles in clay rock, the clay rock sample has to be abraded in thin layers.[14] The actinides are then extracted from the obtained clay powder samples with HNO$_3$. As a consequence of the desorption procedure, a variety of clay matrix elements also dissolve. To simulate such a matrix, to each matrix type A sample actinide tracers were added gravimetrically and mixed with 5 mL of 1 mol L^{-1} HNO$_3$. All samples were prepared at room temperature and under aerobic conditions. The suspensions were left in centrifuge tubes (Sarstedt AG & Co. KG, Nümbrecht, Germany) for 7 d and were occasionally shaken. Subsequently, the samples were centrifuged at 4000 rpm for 10 min (Megafuge 8, Heraeus, Thermo Scientific, Dreieich, Germany) and the supernatants were then processed for the AMS analysis. The samples of matrix type B were acidified with 5 mL of 1 mol L^{-1} HNO$_3$ and the actinide tracer solutions were added. The as-obtained sample solutions from matrix type A, as well as the samples with type B and C matrices, undergo the same steps of chemical preparation for the AMS analysis, as described in the text below.

1 mL of a 3.2 mg mL^{-1} FeCl$_3$ solution (prepared from iron powder, mentioned in the "Materials" section), was added to each sample of matrix types A, B, and C. This resulted in an Fe concentration of 290 mg L^{-1}. Afterwards, a solution of 25% NH$_3$ was added dropwise, while gently shaking the centrifuge tube in order to obtain a brownish precipitate of Fe(OH)$_3$ with which the actinides were co-precipitated. After 1 day, the suspensions were centrifuged for 10 min at 4000 rpm. Afterwards, the supernatants were discarded and the Fe(OH)$_3$ precipitates were washed twice with 5 mL of a 0.05% NH$_3$ solution. Finally, a few drops of 0.05% NH$_3$ solution were added and the wet precipitates were transferred to Eppendorf tubes (Eppendorf Safe-Lock, 0.5 mL, Eppendorf GmbH, Germany). The samples were

Table 1   Overview of sample sets and corresponding compositions regarding the mass of clay rock, volume of synthetic pore water and quantity of actinide nuclides

Sample set	Clay rock/mg	Pore water/mL	Actinide nuclides/(mol per sample)
(i) Sensitivity test samples			$\approx 3 \times 10^{-19}$, 4×10^{-18}, 3×10^{-17}, 4×10^{-16}, or 5×10^{-15}
Matrix type A	100	—	
(ii) Concentration test samples			$\approx 3 \times 10^{-19}$ to 4×10^{-15a}
Matrix type A	100	—	
Matrix type B	—	20	
(iii) Matrix test samples			$\approx 5 \times 10^{-16}$
Matrix type A	100	—	
Matrix type B	—	20	
Matrix type C	—	—	
(iv) Blank samples			—
Matrix type A	100	—	

^{a} Resembling relative solubility concentrations (Table 2).

Table 2 Calculated solubility concentrations of U, Np, Pu, Am, and Cm in their respective dominant oxidation states in OPA and COx pore water and actinide amounts added to concentration test samples (see section 4, "Concurrent determination of actinides in clay systems over several orders of magnitude") prepared in the frame of this work

Actinide	Actinide concentration in OPA/(mol L^{-1})	Actinide concentration in COx/(mol L^{-1})	Actinide amounts added to OPA; COx concentration test samples/ (mol per sample)
U$_{total}$	1.2×10^{-6}	4.0×10^{-7}	$\approx 3.7 \times 10^{-15}$; 2.4×10^{-17}
U(IV)	3.2×10^{-9}	3.2×10^{-9}	
U(VI)	1.1×10^{-6}	4.0×10^{-7}	
Np$_{total}$	1.1×10^{-9}	1.2×10^{-9}	$\approx 2.1 \times 10^{-18}$; 4.6×10^{-19}
Np(IV)	1.1×10^{-9}	1.2×10^{-9}	
Np(V)	9.7×10^{-15}	5.7×10^{-15}	
Pu$_{total}$	5.3×10^{-10}	1.4×10^{-8}	$\approx 2.8 \times 10^{-19}$; 2.7×10^{-18}
Pu(III)	5.2×10^{-10}	1.4×10^{-8}	
Pu(IV)	1.6×10^{-11}	2.1×10^{-11}	
Am(III)	2.0×10^{-6}	3.0×10^{-6}	$\approx 2.9 \times 10^{-15}$; 2.4×10^{-16}
Cm(III)	1.9×10^{-6}	3.0×10^{-6}	$\approx 2.8 \times 10^{-16}$; 1.8×10^{-17}

centrifuged for 5 min at 4000 rpm and the remaining supernatants were discarded. The Fe(OH)$_3$ precipitates were dried at 80 °C for 4 h, transferred into quartz crucibles and converted to Fe$_2$O$_3$ in a furnace (Nabertherm P330, Nabertherm, Lilienthal, Germany) at 800 °C for 3 h. The obtained Fe$_2$O$_3$ pins, each with a total mass of a few mg and a diameter of approximately 1 mm, were pressed into sample holders suited for the AMS 3 MV tandem accelerator VERA (Vienna Environmental Research Accelerator, Vienna, Austria).[1]

The actinide nuclides were measured by setting the terminal voltage at 1.65 MV and choosing the 3+ charge state after stripping with helium, following the procedure described by Winkler *et al.* (2015).[15] The count rates of the five actinide nuclides, ^{233}U, ^{237}Np, ^{244}Pu, ^{243}Am, and ^{248}Cm, were sequentially measured from the same sample according to the multi-actinide analysis method.[3] In the present study, since the total amount of any actinide nuclide in a sample was known, the measuring time dedicated to each nuclide was accordingly defined *a priori* and further adjusted during the measurement as approximately inversely proportional to the square root of its count rate. This allowed for optimizing the duration of the measurement of all nuclides in a sample and reducing the difference in the relative uncertainty due to counting statistics between the count rate of nuclides whose concentration differs by orders of magnitude.[2] Tuning samples containing the in-house reference material for uranium, Vienna-KkU,[16] with a ^{236}U/^{238}U isotopic ratio of $(6.98 \pm 0.32) \times 10^{-11}$ were measured in regular intervals in order to correct for variations in the efficiency of detection. Particular care was taken in determining the background levels of the actinides and their origin. To this purpose, the samples were periodically alternated in the measurement sequence with four procedural blanks. Furthermore, the investigated masses, 233 u, 237 u, 244 u, 243 u, and 248 u were scanned in a sample containing an iron–graphite mixture which can be considered as an instrumental blank, which was provided by VERA. In that way, the contribution of a possible background from the ion source can be identified separately from the background of the procedural blanks.

The aforementioned additional 6 procedural blank samples (three samples per clay type) were analysed for the elemental compositions of (a) the supernatants resulting after the simulated desorption, (b) the supernatants resulting after Fe(OH)$_3$ co-precipitation, and (c) the respective washing solutions. In this way, the co-precipitation efficiencies of natural analogues for the studied actinide tracers were investigated, *i.e.*, ^{238}U(VI) for ^{233}U(VI), ^{232}Th(IV) for ^{237}Np(IV) and ^{244}Pu(IV), and La(III), Ce(III), and Eu(III) for ^{243}Am(III) and ^{248}Cm(III). The overall matrix contents of the AMS targets were estimated by determining the co-precipitation efficiencies of the matrix elements, too, such as Na, Ca, and Al, as well as by weighing of the Fe$_2$O$_3$ pins.

The above-mentioned supernatant and washing solutions were analysed with a quadrupole ICP-MS (XSERIES 2 Quadrupole ICP-MS, Thermo Fisher Scientific, Schwerte, Germany). For calibration, we used the certified reference standard SPS-SW2 (Spectrapure Standards as, P.O. Box 190 Manglerud, Oslo, Norway) containing 45 metal elements with concentrations ranging from 2.5 ng mL^{-1} to 10 μg mL^{-1}.

2.5 Chemical-ionization-yield (CIY) factor

The determined count rates of the five actinide nuclides in the matrix test samples were compared with their added amounts in order to estimate the chemical-ionization-yield (CIY) factors. The ionization yield indicates the fraction of an element in the AMS target that is sputtered as negative ions in the ion source. It was observed in previous studies[3,17,18] that different actinides do not exhibit the same ionization yield during an AMS measurement. Generally, these studies show that the ionization yield increases with the atomic number of the actinide element. The chemical yield indicates which fraction of an element is recovered after the several steps of sample preparation, such as an Fe(OH)$_3$ co-precipitation. Since in the frame of an AMS analysis it is not possible to discriminate between the ionization yield and chemical yield, the CIY is used, representing a combination of both phenomena. However, as already mentioned in the previous section, the chemical yields of the actinides were estimated by determining the yields of natural analogues (*e.g.* Th and U) in the Fe(OH)$_3$ precipitates.

In order to evaluate the relative efficiency of the analysis of an actinide nuclide with respect to another one, the CIY can be estimated with the formula in eqn (1), shown as an example for ^{237}Np and ^{244}Pu:

$$\text{CIY}\left(^{237}\text{Np}/^{244}\text{Pu}\right) = \frac{(\text{ctr}^{237}\text{Np}/\text{ctr}^{244}\text{Pu})}{(\text{N}^{237}\text{Np}/\text{N}^{244}\text{Pu})} \quad (1)$$

where ctr $[\text{s}^{-1}]$ is the count rate and $N\,[–]$ is the nominal number of atoms.

3 Results and discussion

3.1 Solubility and speciation of U, Np, Pu, Am, and Cm

As mentioned in "Experimental", Section 2, before the preparation of the concentration test samples, solubility and speciation calculations were carried out. In the following, the results of these calculations will be commented in terms of the speciation of the actinides in the chosen clay systems, in order to elucidate the expected concentration ranges of the several actinide species. The most influencing parameters of the solubility of the actinides, and consequently, their aqueous speciation, are pH, redox potential and the carbonate concentration of the clay pore water. The dominating aquatic species of the actinides in both OPA and COx pore water were calculated to be their hydroxo and carbonato complexes (ESI Table S2†), with contributions of sulphate and silicate complexes in the cases of Pu and Am, respectively. The as-calculated solubility concentrations ranged from approximately 10^{-11} mol L^{-1} to 10^{-6} mol L^{-1} (Table 2).

For Am and Cm, the only relevant oxidation state was +III with solubility concentrations of approximately 10^{-6} mol L^{-1}, while for Np, the dominant oxidation state was +IV with a solubility concentration of approximately 10^{-9} mol L^{-1} in both pore waters. For U and Pu, the maximum concentrations were very sensitive to small changes of pH and carbonate concentration of the two pore water systems which stabilize the redox state +VI and +III in U and Pu, respectively. In the case of Pu, a solubility concentration of $\approx 5 \times 10^{-10}$ mol L^{-1} was calculated for OPA pore water, which was lower by a factor of 25 as compared to COx pore water ($\approx 10^{-8}$ mol L^{-1}).

This is due to the fact that COx pore water is more reducing, and has a lower pH and higher carbonate concentration, consequently increasing the concentration of Pu(III), which forms soluble carbonato complexes. Pu(IV) is present as

Table 4 Background and respective statistical uncertainty σ_{ctr} of each nuclide

	^{233}U	^{237}Np	^{244}Pu	^{248}Cm
Background/(h^{-1})	0.34	1.76	1.75	5.58
σ_{ctr}/(h^{-1})	0.35	0.79	0.78	1.39

Pu(OH)$_4$(aq) to a lesser extent in both clay systems. In the case of U, the +VI oxidation state is by far the most abundant in aqueous solution. U shows a 3 times higher solubility concentration ($\approx 10^{-6}$ mol L^{-1}) in OPA pore water as in COx pore water ($\approx 4 \times 10^{-7}$ mol L^{-1}), since OPA has higher pH and the pore water contains more calcium. Hence, the formation of U(VI) carbonato complexes with stoichiometries Ca$_{2-x}$UO$_2$(CO$_3$)$_3^{-2x}$ (with $0 \leq x \leq 2$) is favored, increasing the solubility of U.[19] A smaller fraction of the soluble U species is due to U(IV) forming U(OH)$_4$ (aq).

3.2 Determination of the background

For the determination of the background levels of the actinide nuclides four procedural blank samples were analysed. In Table 3, the measurement times and numbers of counts in each procedural blank are reported for the investigated nuclides ^{233}U, ^{237}Np, ^{244}Pu, and ^{248}Cm. The masses were analysed for a total measurement time ranging from 1431 s for ^{237}Np in COx Blank II to 3691 s for ^{244}Pu, as well as ^{248}Cm in OPA Blank II. The four investigated procedural blanks showed very low count rates (ctrs) for all actinide nuclides. In some cases, no counts were detected.

The quantification of the background of each individual actinide nuclide was performed as follows: the numbers of counts (cts [–]) and the respective measurement times [s] in all four blank samples were summed up. Such combination of the numbers of counts of the four blank samples was possible, since OPA and COx clay rock have similar elemental compositions. Then, the uncertainty of the numbers of counts of each nuclide was determined. Given that the counting of signals obeys the Poisson distribution, the Poisson uncertainty (σ_P [–]) of the numbers of counts was estimated according to eqn (2):

$$\sigma_P = \sqrt{\text{cts}} \quad (2)$$

Table 3 Measurement times and numbers of counts for masses 233 u, 237 u, 244 u, and 248 u in blank samples

	OPA Blank I	OPA Blank II	COx Blank I	COx Blank II	Sum
Measurement time for ^{233}U/s	3690	3647	1477	1476	10290
Number of counts for ^{233}U	0	0	1	0	1
Measurement time for ^{237}Np/s	3688	3641	1474	1431	10233
Number of counts for ^{237}Np	2	1	2	0	5
Measurement time for ^{244}Pu/s	3689	3691	1476	1451	10307
Number of counts for ^{244}Pu	1	4	0	0	5
Measurement time for ^{248}Cm/s	3683	3691	1476	1476	10328
Number of counts for ^{248}Cm	2	4	4	6	16

1700 | *J. Anal. At. Spectrom.*, 2022, **37**, 1696–1705

This journal is © The Royal Society of Chemistry 2022

Subsequently, the sum counts and the sum measurement times for each of the four nuclides were divided by each other and multiplied by 3600 s, giving the background as average ctr [h^{-1}] (Table 4).

In order to determine the statistical uncertainty (σ_{ctr} [h^{-1}]) of such average ctr, the uncertainty of the number of counts (σ_P) was divided by the sum measurement time (t_{sum} [s]), as shown in eqn (3):

$$\sigma_{ctr} = \frac{\sigma_P}{t_{sum}} \tag{3}$$

The determined background levels and their respective uncertainties are presented in Table 4.

As can be seen, the background ctr of ^{248}Cm is equal to (5.58 $\pm$ 1.39) h^{-1} and about 16 times higher than that observed for ^{233}U and about 3 times higher than that of ^{237}Np and ^{244}Pu. Such increased background may be explained by the existence of molecular interference during the low energy AMS measurement of mass 248 u in the 3+ charge state, as previously investigated by Christl et al. (2014).[17] These authors demonstrated how this background might be actually caused by the not complete destruction of the quite stable diatomic cation (^{232}Th^{16}O)$^{3+}$ during the He stripping process in the tandem accelerator. This phenomenon can be considered a likely explanation for the observed background at mass 248 u also in the actual study, given the presence of naturally occurring ^{232}Th in the samples with matrix type A (determined with ICP-MS and equal to around 0.36 and 0.16 μg per sample in OPA and COx, respectively) and considering the high efficiency of co-precipitation of Th with Fe(OH)$_3$ as will be described in Section 7 ("Efficiency of the Fe(OH)$_3$ co-precipitation"). It is important to note that the observed level of background does not significantly impair the sensitivity in the analysis of ^{248}Cm, since it is consistent with a concentration of ^{248}Cm of about 4 $\times$ 10^{-19} mol per sample, as will be discussed in the following section ("Sensitivity and performance of AMS in clay systems").

3.3 Sensitivity and performance of AMS in clay systems

The results of the sensitivity test samples are depicted in Fig. 1. Each plot represents the ctr as a function of the nominal amount of ^{233}U, ^{237}Np, ^{244}Pu, and ^{248}Cm in the five different AMS targets (denoted as "sample 1" to "sample 5"), and each of which contains approximately the same amounts of the four actinide nuclides. The ctr of each actinide nuclide increased with increasing nominal amount of nuclides in both OPA and COx samples.

It was observed that this increase in ctr was not linear with respect to the relative nominal amount of an actinide nuclide.

Such non-linearity can arise from the fact that different AMS targets may exhibit up to 50% variability in the ctr for a given amount of nuclide.[20]

The ctrs ranged from a minimum of 2.4 $\pm$ 1.6 h^{-1} (nominal 3 $\times$ 10^{-19} mol ^{244}Pu in COx) to a maximum of (1.02 $\pm$ 0.03) $\times$ 10^4 h^{-1} (nominal 4 $\times$ 10^{-15} mol ^{248}Cm in OPA). The ctrs of ^{237}Np, ^{244}Pu, and ^{248}Cm in COx with a nominal amount of ≈4 $\times$ 10^{-19} mol per nuclide were consistent with the background,
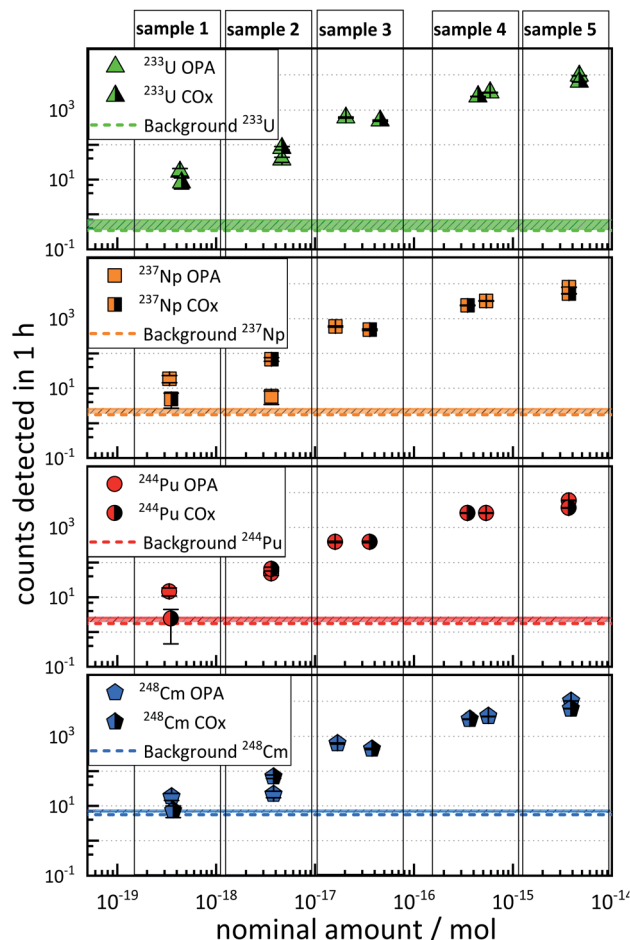

Fig. 1 Sensitivity test samples: counts of ^{233}U, ^{237}Np, ^{244}Pu, and ^{248}Cm in OPA and COx, detected in 1 h, as a function of the nominal amounts of actinide nuclides in the clay rock samples. The background for each nuclide is indicated as a solid horizontal line. The statistical uncertainties of the nominal amounts of nuclides were ≤5%.

indicated as dashed horizontal lines in Fig. 1. The ctrs in samples with nominal nuclide amounts of ≈4 $\times$ 10^{-18} mol or more were significantly higher than the background, except for 4 $\times$ 10^{-18} mol ^{237}Np in OPA. In this case, the ctr was even lower than for a nominal amount of 3 $\times$ 10^{-19} mol. This observation might be explained by an exceptionally low chemical yield of ^{237}Np.

It can be stated that an accurate determination of ^{233}U, ^{237}Np, ^{244}Pu, and ^{248}Cm was possible in matrix type A down to levels of approximately 4 $\times$ 10^{-18} mol, since the determination of nominal amounts of approximately 4 $\times$ 10^{-19} mol per nuclide was, in some cases, hampered by a similarly high ctr in the blank samples.

3.4 Concurrent determination of actinides in clay systems over several orders of magnitude

This section illustrates the results from the concentration test samples (described in "Experimental", Section 3.2), aiming at the simulation of clay and pore water samples from experiments possibly involving the concurrent diffusion of ^{233}U, ^{237}Np,

This journal is © The Royal Society of Chemistry 2022

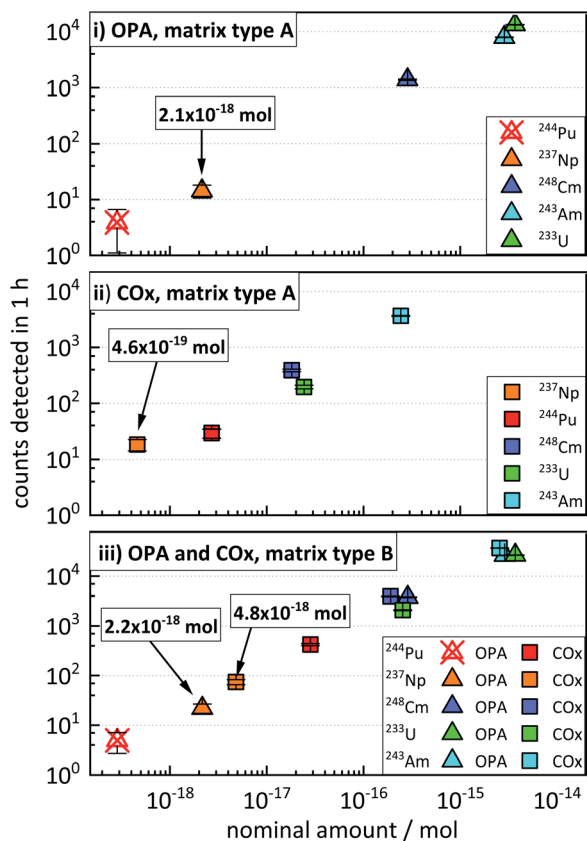J. Anal. At. Spectrom., 2022, 37, 1696–1705 | 1701

Fig. 2 Concentration test samples: number of counts detected in 1 h for each actinide nuclide in (i) OPA, matrix type A, (ii) COx, matrix type A, and (iii) OPA and COx, matrix type B, as a function of the nominal amount of each actinide nuclide. Crossed out data points represent ctrs consistent with the background.

^{244}Pu, ^{243}Am, and ^{248}Cm. The data presented in Fig. 2 show an increase in the average ctr of each actinide nuclide with increasing nominal amount of nuclides in the four concentration test samples. The ctrs ranged from a minimum of 3.9 ± 2.1 h^{-1} for ^{244}Pu in OPA (matrix type A) (Fig. 2i) to a maximum of $(3.68 \pm 0.04) \times 10^4$ h^{-1} for ^{243}Am in COx (matrix type B) (Fig. 2iii). The ctrs of ^{244}Pu in OPA matrix type A and matrix type B were consistent with the background (Fig. 2i and iii). The ctr for a certain nominal amount of nuclides in samples of matrix type B was significantly higher, than in samples of matrix type A. For instance, for a nominal amount of $\approx 4 \times 10^{-15}$ mol of ^{233}U in OPA matrix type A, a ctr of $(1.33 \pm 0.02) \times 10^4$ cts h^{-1} was determined, while for matrix type B, a ctr $(2.66 \pm 0.03) \times 10^4$ h^{-1} was obtained. This behaviour can be explained by a dilution effect during the sputtering of the AMS target in the AMS ion source, as will be discussed in the following Section 5 ("Influence of the sample matrix on the efficiency of the analytical method"). The determination of actinide nuclides in matrix type A samples was possible down to $(2.1 \pm 0.6) \times 10^{-18}$ mol in OPA and $(4.6 \pm 1.1) \times 10^{-19}$ mol in COx, respectively. In matrix type B samples actinide nuclides were determined down to $(2.2 \pm 0.5) \times 10^{-18}$ mol in OPA and $(4.8 \pm 0.6) \times 10^{-18}$ mol in COx, respectively.

These results show that multi-actinide analysis can be successfully applied to the concurrent determination of ultra-trace amounts of the five actinide nuclides in the same sample, with relative nuclide quantities covering more than three orders of magnitude.

3.5 Influence of the sample matrix on the efficiency of the analytical method

The matrix test samples contained the nuclides ^{233}U, ^{237}Np, ^{244}Pu, ^{243}Am, and ^{248}Cm, each with a nominal concentration of about 5×10^{-16} mol per sample.

As already described in the previous section, matrix type A samples, having the highest matrix content, exhibited the lowest ctrs, while samples of matrix type B showed approximately three times higher ctrs. Samples of matrix type C, having
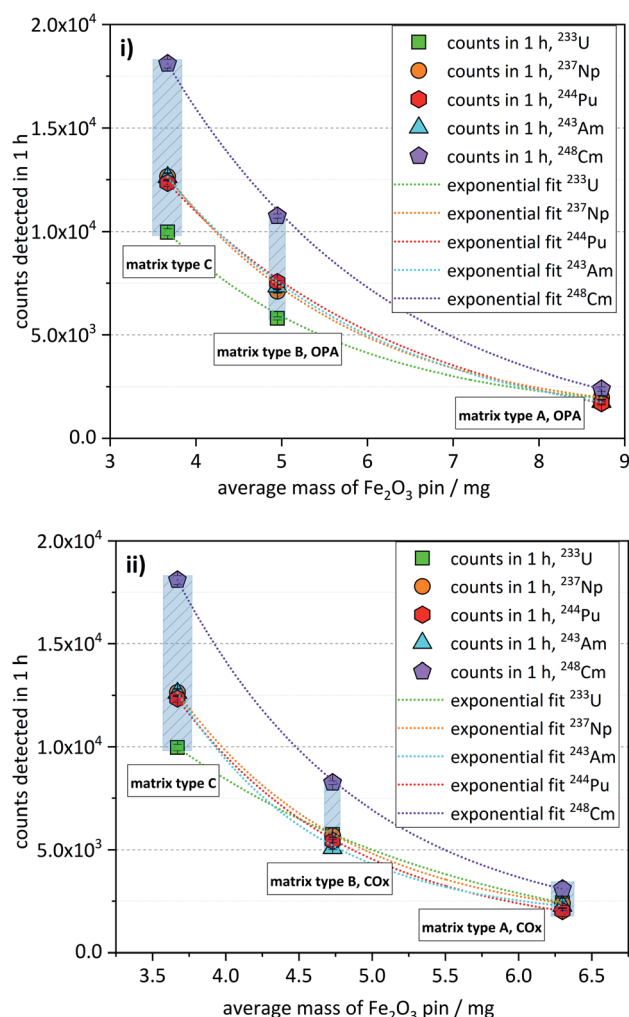

Fig. 3 Matrix test samples: number of counts detected in 1 h for each of the investigated actinide nuclides (nominal amount $\approx 5 \times 10^{-16}$ mol per sample per nuclide) in Fe$_2$O$_3$ pins containing matrix type A, matrix type B, and matrix type C for (i) OPA and (ii) COx, given as a function of the average mass of the corresponding Fe$_2$O$_3$ pins (uncertainties of the average masses are indicated as blue shaded areas).

Table 5 Average masses of Fe_2O_3 pins of matrix types A, B, and C. Each mean value was obtained by weighing three Fe_2O_3 pins

	Matrix type A: OPA	Matrix type A: COx	Matrix type B: OPA	Matrix type B: COx	Matrix type C
Mass/(mg)	8.73 ±0.05	6.30 ±0.22	4.95 ±0.11	4.73 ±0.12	3.67 ±0.17

Table 6 CIY values for a selection of nuclide pairs given for all investigated matrices of the matrix test samples, as well as the respective average CIY

	$^{237}Np/^{244}Pu$	$^{248}Cm/^{243}Am$	$^{248}Cm/^{233}U$
Matrix type A, OPA	1.2 ± 0.1	1.3 ± 0.1	1.3 ± 0.2
Matrix type A, COx	1.2 ± 0.1	1.3 ± 0.2	1.6 ± 0.2
Matrix type B, OPA	0.94 ± 0.04	1.34 ± 0.05	2.24 ± 0.09
Matrix type B, COx	1.04 ± 0.04	1.49 ± 0.05	1.74 ± 0.06
Matrix type C	1.04 ± 0.03	1.33 ± 0.04	2.02 ± 0.07
Average CIY	1.1 ± 0.1	1.32 ± 0.08	1.7 ± 0.4

the lowest matrix content, showed the highest ctrs, being up to 6 times higher compared with matrix type A (Fig. 3). This trend is shown for both OPA (Fig. 3i) and COx matrices (Fig. 3ii). As can also be seen in Fig. 3, there is a non-linear, but rather a somewhat exponential correlation between the ctr of a nuclide and the average mass of the corresponding Fe_2O_3 pin (listed in Table 5).

As will be described in Section 7 ("Efficiency of the $Fe(OH)_3$ co-precipitation"), the co-precipitation of some matrix elements, like Al and Ca, may be significant and increase the mass of the Fe_2O_3 pin. In this way, the observed trend of decreasing ctrs with increasing mass of the Fe_2O_3 pin can be attributed to the corresponding matrix content of the AMS target.

The phenomenon depicted in Fig. 3 can be interpreted as an increase of overall detection efficiency, with decreasing matrix content. The overall detection efficiency is expressed here as an unambiguous number of events counted in the detector per atom of a certain actinide nuclide in the sample during one-hour measurement. The observed trend can be explained considering that in the ion source of the high-intensity Multi-Cathode Source for Negative Ions by Cesium Sputtering type (MC-SNICS),[21] used at VERA, a similar sputter rate typically of several mono-layers per second[22] can be assumed for all the samples that are analyzed during the same measurement run. The sputtering rate of the actinide nuclides during this process would be lower in the AMS targets with a higher matrix compared to those with a lower matrix but with the same content of actinide nuclides, in a process that could be described as a dilution effect on the observed ctr of the actinides.

A further influence of certain matrix elements on the ionization efficiency of the actinide nuclides cannot be explained by the actual experiment and a more extensive study should be carried out in order to identify such phenomena. Finally, the authors can exclude a dependency of the chemical yield of the $Fe(OH)_3$ co-precipitation of the actinide nuclides on the matrix of the sample, since this has been proven to be quantitative for matrix type A samples, as will be described in Section 7.

3.6 Investigation of non-isotopic tracers

The suitability of non-isotopic tracers was investigated by comparing the CIY factors of several pairs of actinide nuclides and their variation in different matrices (Table 6). The CIY factors were estimated based on the ctrs of the matrix test samples (Section 5) and eqn (1). The average CIY factors ranged from 1.1 ± 0.1 (for $^{237}Np/^{244}Pu$) to 1.7 ± 0.4 (for $^{248}Cm/^{233}U$). The variation was more pronounced for nuclides with strongly

Table 7 Selection of matrix elements present in OPA and COx and corresponding fractions co-precipitated with $Fe(OH)_3$ directly after co-precipitation and recoveries after washing steps, determined as average of three blank samples per clay type each

	Fraction co-precipitated with $Fe(OH)_3$/%		Fraction present in the $Fe(OH)_3$ precipitate, after the 1st washing step/%		Fraction present in the $Fe(OH)_3$ precipitate, after the 2nd washing step/%	
Element	OPA	COx	OPA	COx	OPA	COx
Na(I)	11.1 ± 0.5	1.7 ± 0.1	9.7 ± 0.6	0.8 ± 0.2	8.8 ± 0.7	0.8 ± 0.2
K(I)	16.5 ± 0.5	9.6 ± 0.1	10.6 ± 1.1	9.6 ± 0.1	4.8 ± 1.7	9.6 ± 0.1
Mg(II)	20.1 ± 0.9	15.6 ± 0.5	16.3 ± 1.7	11.4 ± 1.4	15.2 ± 2.0	11.2 ± 1.4
Ca(II)	19.7 ± 0.8	14.1 ± 0.2	16.2 ± 1.5	10.2 ± 1.0	15.1 ± 1.7	10.0 ± 1.7
Sr(II)	25.3 ± 1.7	20.4 ± 0.7	22.4 ± 2.3	16.7 ± 1.5	21.5 ± 2.5	16.5 ± 1.6
Al(III)	99.8 ± 4.2	98.2 ± 2.5	97.8 ± 4.9	97.1 ± 3.1	96.1 ± 5.3	94.7 ± 3.8
Fe(III)	99.9 ± 1.9	99.8 ± 1.3	99.5 ± 2.0	99.5 ± 1.4	99.4 ± 2.1	99.4 ± 1.5
La(III)	99.0 ± 3.7	99.7 ± 2.2	98.5 ± 3.8	99.4 ± 2.4	98.3 ± 4.0	99.2 ± 2.5
Ce(III)	99.5 ± 3.4	99.8 ± 3.4	99.2 ± 3.6	99.6 ± 3.5	99.1 ± 3.7	99.5 ± 3.6
Eu(III)	98.3 ± 3.9	96.8 ± 3.2	97.1 ± 4.0	94.6 ± 3.4	95.8 ± 4.1	92.5 ± 3.6
$^{232}Th(IV)$	99.8 ± 2.8	99.5 ± 3.2	99.4 ± 3.1	99.2 ± 3.4	99.3 ± 3.1	98.9 ± 3.4
$^{238}U(VI)$	96.6 ± 3.4	95.2 ± 4.1	94.1 ± 3.7	91.8 ± 4.4	91.6 ± 3.9	88.5 ± 4.7

different chemical characteristics, for instance, ^{248}Cm/^{233}U (CIY = 1.3 ± 0.02 to 2.24 ± 0.09), while it was less distinct for nuclides, which are chemically more similar, for instance ^{237}Np/^{244}Pu (CIY = 0.94 ± 0.04 to 1.22 ± 0.1) and ^{248}Cm/^{243}Am (CIY = 1.3 ± 0.1 to 1.49 ± 0.05). It can be assumed that the relative behaviours of two nuclides to each other—both during AMS sample preparation and during sputtering in the AMS ion source—are less affected by the sample matrix if the two nuclides share similar chemical properties. These results show that in clay matrices ^{244}Pu can be used for ^{237}Np as a non-isotopic tracer as well as ^{248}Cm for ^{243}Am, respectively, with relative standard deviations from 8 to 10% in their CIY factors, as observed in the actual study.

3.7 Efficiency of the Fe(OH)$_3$ co-precipitation

Element concentrations and the derived co-precipitation efficiencies described in this section are expressed as average values obtained from the analysis of three separate samples per clay type. In the procedural blank samples of both clay types, more than 99% of Fe (desorbed from clay rock + added as FeCl$_3$), initially dissolved in the acidic extract, was recovered in the Fe(OH)$_3$ precipitate, as shown in Table 7. Hence, the Fe(OH)$_3$ precipitation was quantitative. Furthermore, the two washing steps of the precipitate did not significantly affect the stability of the Fe(OH)$_3$ precipitate, since the concentration of re-dissolved Fe in the washing solution was negligible. In fact, the fraction of Fe present in the Fe(OH)$_3$ precipitate after each washing step was less than 1% lower compared to the initial precipitate.

Elements listed in Table 7 with oxidation states +III and higher were quantitatively co-precipitated with Fe(OH)$_3$. In particular, the naturally occurring lanthanides, such as La(III) and Ce(III) which serve as chemical analogues of ^{243}Am(III) and ^{248}Cm(III), and Th(IV) as an analogue of ^{244}Pu(IV), show a co-precipitation efficiency of about 99% and also negligible re-dissolution during the two washing steps. Eu(III) shows a somewhat lower efficiency for its co-precipitation with Fe(OH)$_3$ with a value of (96.8 ± 3.2)% for, *e.g.*, the blanks containing the COx clay matrix and a higher degree of re-dissolution in the two washing steps, down to (92.5 ± 3.6)%, for the same blanks, accounting for around 4.3% of the amount of Eu(III) initially co-precipitated. Such a value is, however, consistent with the statistical uncertainty of the aforementioned efficiencies. A similar trend was observed for the naturally occurring ^{238}U(VI) with an initial co-precipitation efficiency of (96.6 ± 3.4)% and (95.2 ± 4.1)%, for the blanks containing OPA and COx clay, respectively, and a subsequent re-dissolution after the two washing steps of 5% and 5.6%, respectively. Also in this case, the fraction of re-dissolved U(VI) is consistent within the statistical uncertainties. The very high efficiency (≥95%) for the final co-precipitation of Al(III) with Fe(OH)$_3$ implies that an amount of Al equal to approximately 436 and 132 µg, for the OPA and COx blanks respectively, is to be found in the Fe$_2$O$_3$ pin of the AMS target. As shown in Table 7, the mono and divalent matrix elements (*i.e.* Na, K, Mg, Ca, and Sr) were not quantitatively co-precipitated. In fact, after the second washing step,

Table 8 Selection of elements present in OPA and COx and their corresponding initial concentrations in the desorption solution, determined as average of three blank samples per clay type each

Element	Initial concentration in desorption solution/(mg L^{-1})	
	OPA	COx
Na(I)	$(2.02 \pm 0.08) \times 10^1$	$(9.68 \pm 0.02) \times 10^0$
K(I)	$(1.65 \pm 0.04) \times 10^1$	$(1.19 \pm 0.02) \times 10^1$
Mg(II)	$(6.5 \pm 0.2) \times 10^1$	$(3.08 \pm 0.02) \times 10^1$
Ca(II)	$(4.8 \pm 0.2) \times 10^2$	$(7.10 \pm 0.03) \times 10^2$
Sr(II)	$(2.1 \pm 0.1) \times 10^0$	$(4.15 \pm 0.09) \times 10^0$
Al(III)	$(6.5 \pm 0.2) \times 10^1$	$(2.00 \pm 0.03) \times 10^1$
Fe(III)^a	$(5.83 \pm 0.01) \times 10^2$	$(4.68 \pm 0.06) \times 10^2$
La(III)	$(4.8 \pm 0.2) \times 10^{-2}$	$(6.1 \pm 0.1) \times 10^{-2}$
Ce(III)	$(1.78 \pm 0.06) \times 10^{-1}$	$(1.19 \pm 0.04) \times 10^{-1}$
Eu(III)	$(5.8 \pm 0.2) \times 10^{-3}$	$(3.3 \pm 0.1) \times 10^{-3}$
^{232}Th(IV)	$(5.2 \pm 0.1) \times 10^{-2}$	$(2.29 \pm 0.07) \times 10^{-2}$
^{238}U(VI)	$(2.85 \pm 0.09) \times 10^{-3}$	$(2.15 \pm 0.08) \times 10^{-3}$

^{a} Fe concentrations also include Fe originating from the FeCl$_3$ solution (290 mg L^{-1}) added prior to the Fe(OH)$_3$ precipitation step.

a fraction ≤22% of these elements was recovered in the precipitates. However, even such low co-precipitation efficiencies can significantly contribute to the matrix of the final AMS target. This is particularly relevant for Ca, whose concentration in the acidic extract of the clay samples is at the level of several hundred mg L^{-1} (Table 8) and, in this way, contributed 509 µg (OPA) and 496 µg (COx) to the Fe$_2$O$_3$ pin of the final AMS target.

This experiment indicates that, while a high efficiency of the Fe(OH)$_3$ co-precipitation for the group separation of the tracer actinide nuclides ^{233}U(VI), ^{237}Np(V), ^{244}Pu(IV), ^{243}Am(III), and ^{248}Cm(III) similar to their natural analogues can be assumed, their separation from the matrix elements is only partial and has to be accounted responsible for the significantly higher mass of the AMS targets of samples of matrix type A compared with those of matrix types B and C, as listed in Table 5.

4   Conclusions

The present study demonstrated the analytical capability of AMS in OPA and COx clay matrices by an accurate and sensitive determination of the actinide nuclides ^{233}U, ^{237}Np, ^{244}Pu, and ^{248}Cm down to 3×10^{-19} mol per sample. Even though an up to 6-fold decrease in the ctr of the actinide nuclides was observed in the clay matrix samples compared to the standard ones, that can be attributed to the undesired co-precipitation of some matrix elements with Fe(OH)$_3$, the employed sample preparation procedure presents the advantage of a quantitative co-precipitation of the actinides. This allows for the use of non-isotopic tracers, such as ^{244}Pu for ^{237}Np and ^{248}Cm for ^{243}Am, as demonstrated in this work and, in this way, for the concurrent determination of the investigated actinide nuclides.

It was shown that such concurrent determination of ^{233}U, ^{237}Np, ^{244}Pu, ^{243}Am, and ^{248}Cm, from the same AMS target is also possible in samples in which the investigated nuclides are present at quantities covering more than three orders of

1704 | *J. Anal. At. Spectrom.*, 2022, **37**, 1696–1705

This journal is © The Royal Society of Chemistry 2022

magnitude, down to 5×10^{-19} mol per sample, resembling their relative solubility in clay pore water.

The presented experimental results demonstrate that samples from laboratory diffusion experiments for actinides can be analysed down to concentration levels up to eight orders of magnitude lower as compared to those obtained in the study of Joseph *et al.* (2013)[12] for ^{233}U diffusion through OPA. Furthermore, this study offers the analytical capability of studying the simultaneous diffusion of U, Np, Pu, Am, and Cm through the same clay sample, down to ultra-trace levels. The outcomes of this study pave the way to the still unexplored experimental observation of the diffusion behaviour of actinides at ultra-trace levels through clay rock.

Conflicts of interest

There are no conflicts to declare.

Acknowledgements

References

1 P. Steier, K. Hain, U. Klötzli, J. Lachner, A. Priller, S. Winkler and R. Golser, *Nucl. Instrum. Methods Phys. Res., Sect. B*, 2019, **458**, 82–89.

2 F. Quinto, R. Golser, M. Lagos, M. Plaschke, T. Schäfer, P. Steier and H. Geckeis, *Anal. Chem.*, 2015, **87**, 5766–5773.

3 F. Quinto, I. Blechschmidt, C. Garcia Perez, H. Geckeis, F. Geyer, R. Golser, F. Huber, M. Lagos, B. Lanyon, M. Plaschke, P. Steier and T. Schäfer, *Anal. Chem.*, 2017, **89**, 7182–7189.

4 PHREEQC v.3, **https://wwwbrr.cr.usgs.gov/projects/GWC_cou-pled/phreeqc/**.

5 P. Bossart and M. Thury, *Mont Terri Rock Laboratory – Project, Programme 1996 to 2007 and Results*, 2008.

6 ANDRA, *Evaluation of the Feasibility of a Geological Repository in an Argillaceous Formation*, 2005.

7 F. J. Pearson, *OPALINUS CLAY EXPERIMENTAL WATER: A1 Type, Version 980318*, 1998.

8 S. Savoye, C. Beaucaire, B. Grenut and A. Fayette, *Appl. Geochem.*, 2015, **61**, 41–52.

9 *Thermochimie v.10 Database*, **https://www.thermochimie-tdb.com/**.

10 A. Gautschi, *Grundwasser*, 2017, **22**, 221–233.

11 A. Vinsot, S. Mettler and S. Wechner, *Phys. Chem. Earth*, 2008, **33**, S75–S86.

12 C. Joseph, L. R. Van Loon, A. Jakob, R. Steudtner, K. Schmeide, S. Sachs and G. Bernhard, *Geochim. Cosmochim. Acta*, 2013, **109**, 74–89.

13 P. Steier, F. Dellinger, O. Forstner, R. Golser, K. Knie, W. Kutschera, A. Priller, F. Quinto, M. Srncik, F. Terrasi, C. Vockenhuber, A. Wallner, G. Wallner and E. M. Wild, *Nucl. Instrum. Methods Phys. Res., Sect. B*, 2009, **268**, 1045–1049.

14 L. R. Van Loon and W. Müller, *Appl. Radiat. Isot.*, 2014, **90**, 197–202.

15 S. R. Winkler, P. Steier, J. Buchriegler, J. Lachner, J. Pitters, A. Priller and R. Golser, *Nucl. Instrum. Methods Phys. Res., Sect. B*, 2015, **361**, 458–464.

16 P. Steier, M. Bichler, L. Keith Fifield, R. Golser, W. Kutschera, A. Priller, F. Quinto, S. Richter, M. Srncik, P. Terrasi, L. Wacker, A. Wallner, G. Wallner, K. M. Wilcken and E. Maria Wild, *Nucl. Instrum. Phys. Res., Sect. B*, 2008, **266**, 2246–2250.

17 M. Christl, X. Dai, J. Lachner, S. Kramer-Tremblay and H. A. Synal, *Nucl. Instrum. Methods Phys. Res., Sect. B*, 2014, **331**, 225–232.

18 M. López-Lora and E. Chamizo, *Nucl. Instrum. Methods Phys. Res., Sect. B*, 2019, **455**, 39–51.

19 J. Y. Lee, S. Amayri, V. Montoya, D. Fellhauer, X. Gaona and M. Altmaier, *Appl. Geochem.*, 2019, **111**, 104374.

20 F. Quinto, E. Hrnecek, M. Krachler, W. Shotyk, P. Steier and S. R. Winkler, *Environ. Sci. Process. Impacts*, 2013, **15**, 839–847.

21 C. Vockenhuber, I. Ahmad, R. Golser, W. Kutschera, V. Liechtenstein, A. Priller, P. Steier and S. Winkler, *Int. J. Mass Spectrom.*, 2003, **223–224**, 713–732.

22 R. Middleton, D. Juenemann and J. Klein, *Nucl. Instrum. Methods Phys. Res., Sect. B*, 1994, **93**, 39–51.

This journal is © The Royal Society of Chemistry 2022

J. Anal. At. Spectrom., 2022, **37**, 1696–1705 | **1705**